Chapter II

Theoretical Part

2.1 A macroscopic picture of batch melting

As mentioned in the introduction already, mathematical model -ling (Fuhrmann,1973), (Mase and Oda, 1980), and (Hilbig and Kirmsse, 1986) suggests that batch melting proceeds as a quasi-stationary and quasi-isothermal process during most of the melting time. Then we can treat the batch melting as a heat flow coupled to a mass turnover rate by the thermochemistry of melting reactions, and a mass flow coupled to the mass conversion rate by the fluid mechanics of the generated melt. Therein, the mass turnover acts as a heat sink and a source of drainable matter. The basic idea can be sketched as the figure below.

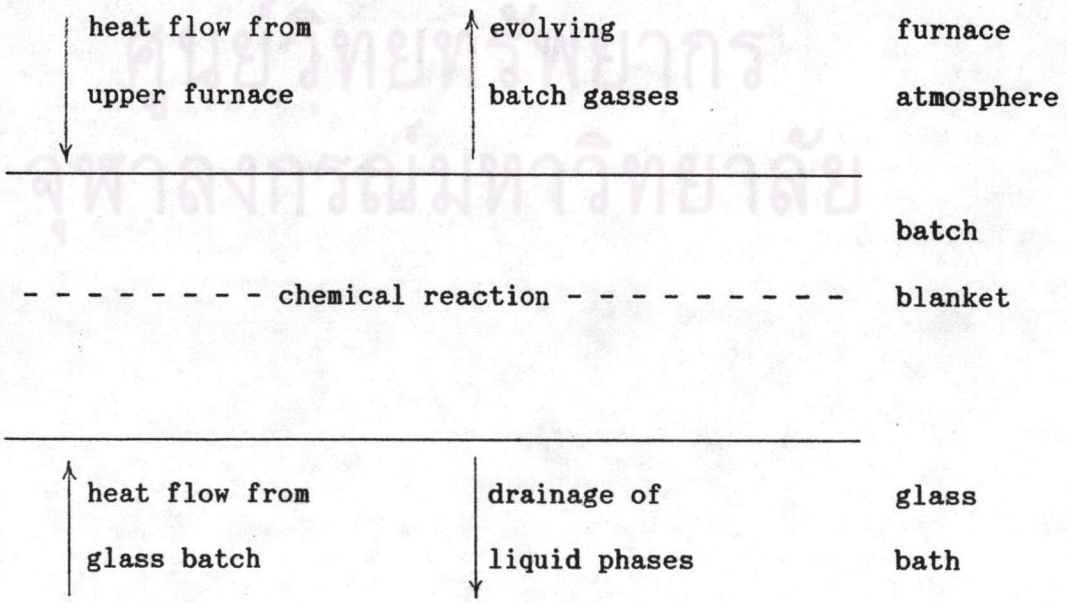

During the first phase of modelling, no discernment is made between the heat flows from below and above, and the amount of heat carried away by the evolving gasses is neglected. The following details were elaborated.

(a) According to previous theoretical work (Fuhrmann, 1973) the batch melting process assumed as a stationary state throughout more than 90 % of the batch melting time, and the batch blanket can be treated as isothermal surface in good approximation (shown in fig. 2.1 and 2.2).

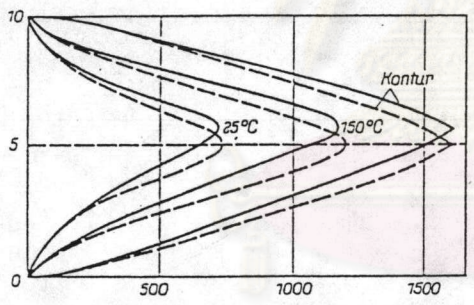

Fig. 2.1 Temperature profile in the batch blanket (Fuhrmann, 1973).

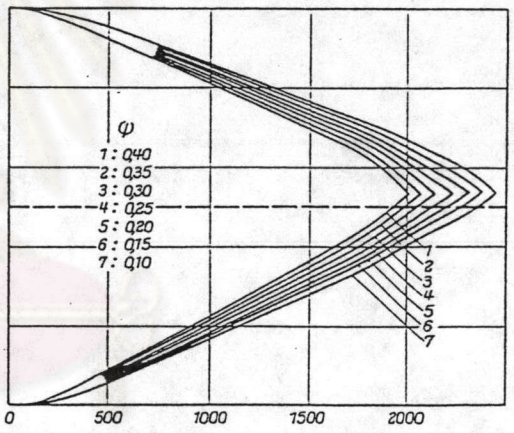

Fig. 2.2 Melting front of batch blanket (Fuhrmann, 1973); ψ is the hypothetical porosity.

In addition to this, we assumed that the batch blanket takes a temperature equal to the liquidus T_R of the resulting glass or subsystem. T_R can be determined by consulting phase diagrams, or by the system given by Backmann et al. (1990). The batch melting thus pro-

ceeds at a constant rate r_b,

$$r_b = (1/A_b) \cdot (dm/dt) = \text{constant}$$

A_b = area of batch blanket, m = mass of primary melt formed

(b) the formation of primary melt consumed a well defined amount of heat H_R (due to the mostly endothermic batch melting reactions) According to Conradt and Phimkhaokham (1990) H_R can be directly derived from the amounts of raw materials in the batch. Written down as a rate equation, this reads

$$r_Q = H_R \cdot r_b$$

r_Q = heat flow rate (sink term) drawn by the batch melting reactions.

(c) The stationary state can be established in different ways. Either r_Q is limited by the heat flow rate r_Q, entering the batch blanket, or r_b is limited by the rate of drainage r_d of primary melt from the batch blanket, or r_b is limited by the overall rate r_R of the chemical reactions. Since in a sequence of consecutive steps, the slowest one determines the overall rate, we may write the batch melting rate as

$$r_b = \text{Min}[r_Q, / H_R; r_d; r_R]$$

The maximal pull rate achievable in a glass melting unit can never

exceed the amount of matter provided by r_b. Taking into account the ratio of blanket area A_b to total melt area A_o, this reads

$$\text{pull} \leq (A_b / A_o) \cdot r_b;$$

as a guide line $A_b/A_o \sim 0.33$

(d) for the heat flow rate r_Q' from the hot environment with $T = T_h$ into the batch blanket with $T = T_R$, different approaches were tried. According to the concept of conduction heat transfer, this can be written as following equation

$$r_Q' = a_{eff} \cdot (T_h - T_R)$$

where a_{eff} is the effective heat transfer coefficient. According to Fuhrmann (1973), a_{eff} range from 40 to 80 W/(m^2 K). Adopting T_h = 1600 °C, T_R = 800 °C, H_R = 140 KWh/t for demonstration purposes yields

$$\text{pull} \leq 0.33\ (r_Q'/H_R) = 1.8 \text{ to } 3.7\ t/(m^2.d)$$

which is in excellent agreement with factory experience. Another approach to determine the heat flow rate is using of radiation heat transfer concept. When a real body emits the radiation flux at an absolute temperature T the heat flow rate due to radiation r_Q'' can be described as

$$r_Q'' = EKT^4$$

when E = emissivity (0<E<1 for a real body) and K = Stefan-Boltzmann constant [K = 5.6697 x 10^{-8} W/(m^2.K^4)]. If a radiation flux q_i is incident on a real body, energy absorbed q_a by the body is given by

$$q_a = aq_i$$

when "a" is the absorptivity which lies between zero and unity. The absorptivity A of a body is generally different from its emissivity E. However, to simplify the analysis, "a" is assumed to equal E. If the batch blanket has surface area A_b, hence, the radiation energy absorbed by a blanket is equal to

$$A_b aKT^4_h$$

then the net radiation at the surface of a blanket is the diffrence between the energy emitted and the energy absorbed.

$$Q_1 = AEKT^4_R - AaKT^4_h$$

For E = a, this result simplifies to

$$Q_1 = AEK(T^4_R - T^4_h)$$

(e) For the drainage rate r_d, the general relation

$$r_d = \rho/v_d$$

v_d = drainage velocity, ρ = density of primary melt.

Among several possible mechanisms for v_d, the surface tension driven velocity was chosen

$$v_d = 6/n$$

6 = surface tension, n = viscosity of primary melt at $T = T_R$. For demonstration purposes, the following data are used. The viscosity of Na_2O-SiO_2 melt at 800 °C, n = 7800 Ns/m^2, the surface tension 6 = 0.3 N/m, the density = 2500 kg/m^3. This yields

$$\text{pull} \leq 0.33\ r_d \sim 2.8\ t/(m^2.d)$$

which also matches with factory experience.

2.2 Thermodynamics of batch melting

2.2.1 Low-liquidus melting of individual raw materials

Liquid phase formation during batch melting is a key event. Therefore, a detailed literature study on the thermodynamics of primary liquid phase formation was performed. Typical batches of the soda lime silicate glasses usually contain low-liquidus compound like Na_2CO_3, Na_2SO_4, and $NaNO_3$. Besides this, Na_2S has to be taken into account as an intermediate low-liquidus product of the sulfate-coal reactions.

$$Na_2SO_4 + 2C \text{ -----> } Na_2S + 2CO_2,$$

$$Na_2SO_4 + 4CO \text{ -----> } Na_2S + 2CO_2.$$

A table 2.1 compiles a number of compounds which may form primary liquid phases by direct melting or with only one raw material involved.

Tab 2.1 Properties of low liquidus melting Na compounds; Molar mass M, liquidus temperature T_{liq}, enthalpy of melting H_{melt}, heat content H_o referred to 25 °C, (after Babuskin, Matveyev, and Mchedlov-Petrossyan, (1985), and Barin and Knacke,(1973)) and viscosity n at $T = T_{liq}$,

compound	M in g/mol	T_{liq} in °C	H_{melt} in KW/t	H_o (1000°C) in KWh/t	log n,n in dPa.s
Na_2CO_3	105.998	851	77.8	424.0	≤ 0
$NaNO_3$	80.995	306	50.1	458.4	≤ 0
Na_2SO_4	142.040	884	66.2	408.5	≤ 0
Na_2S	78.042	1172	93.9	338.0	≤ 0

Binary mixture of the solid melts exhibit very straightforward behavior (see fig. 2.3 a-c). $NaNO_3$ and Na_2SO_4 are easilly dissolved in each other (continuous solution) therby slightly decreasing their liquidus temperatures, however not below 800 °C.

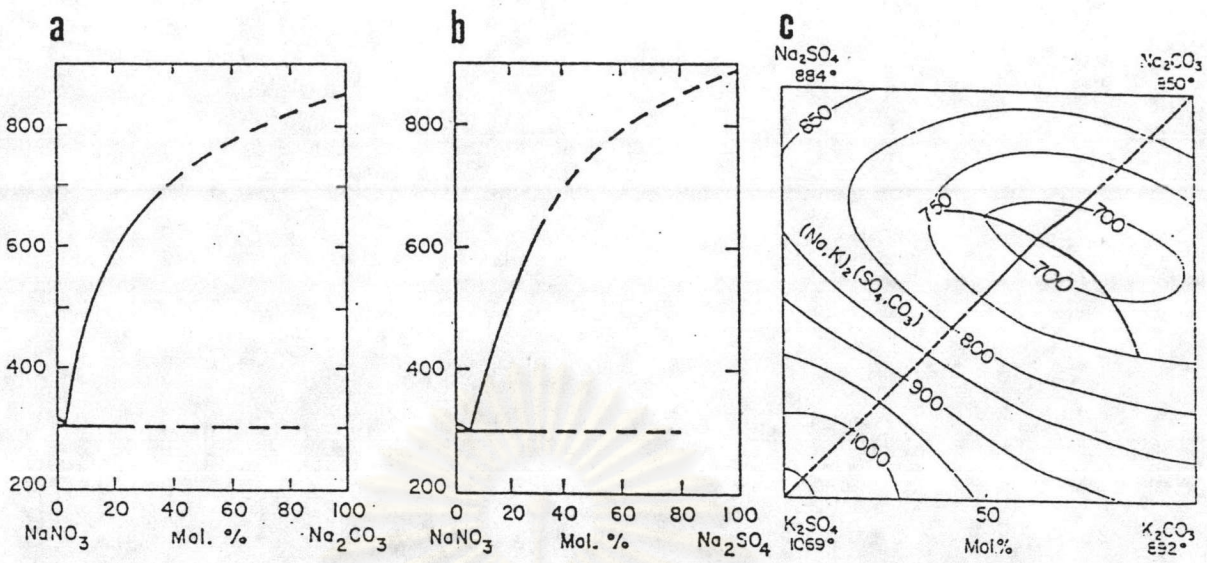

Fig. 2.3 a-c. Phase diagrams of the systems $NaNO_3$-Na_2CO_3 (a), $NaNO_3$-Na_2SO_4 (b), and Na-K-CO_3-SO_4 (c); after Levin, Robin, and Mcmurdie, (1964, 1969).

Primary melt due to sulfate-carbon reaction is also formed well below 1000 °C when an excess of soda ash is present. Phase relation in the system Na-S-O-C is complicated, and until today information is incomplete (see fig. 2.4 and 2.5).

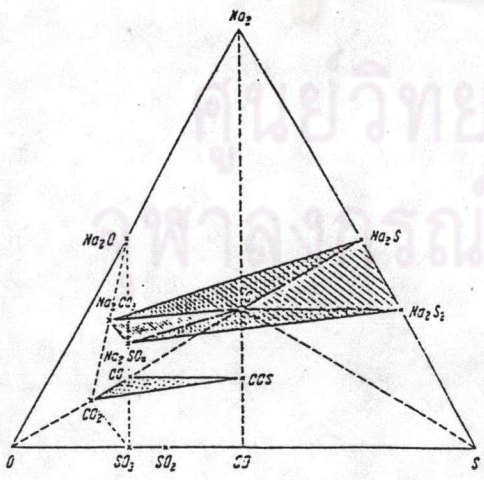

Fig. 2.4 Phase relations in the system Na-S-O-C (after Kroger and Vogel, 1955).

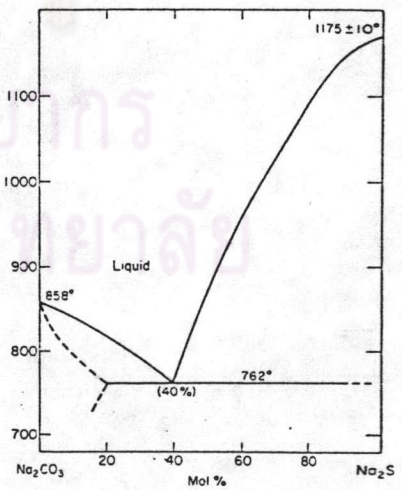

Fig 2.5 Phase relation in the system Na_2CO_3-Na_2S (after Tegman and Warnsqvist, 1972).

2.2.2 The sodium silicate reactions

All of the compounds listed in table 1 strongly react with the quartz in the batch. And this is indeed one of the main courses of batch reactions. With soda ash, the following sequence occurs:

$$Na_2CO_3 + nSiO_2 \text{ -----> } Na_2O.nSiO_2 + CO_2,\ n = 1/2,\ 1,\ 2,\ 3.$$

The two components begin to react precisely from 630 °C upwards and it has been proved (Harinton et al., 1963) that in the 630-780 °C with a 4:1 ratio of components, the reactions proceeds in accordance with the schematic equation

$$Na_2CO_3 + 4SiO_2 \text{ -----> } Na_2SiO_3 + 3SiO_2 + CO_2$$

According to the works by Chedlor, however, reaction in $NS-NS_2$ is predominant. This means that, NS and NS_2 are formed and this is equivalent to n = 1, 2 of the previous equation. The reaction mechanism may be illustrated by means of the model shown in Fig. 2.6.

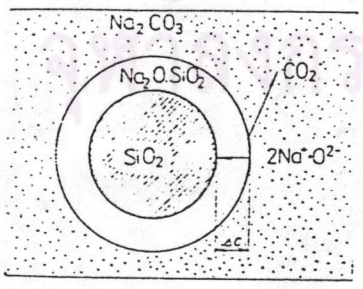

Fig. 2.6 A model for the solid -state reaction between SiO_2 and Na_2CO_3 (Harrington, 1963).

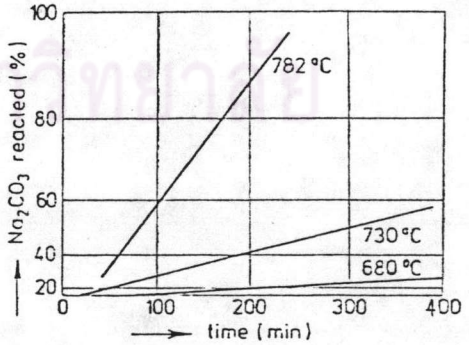

Fig. 2.7 The reaction of SiO_2 (0.06-0.075 mm)with Na_2CO_3 (<0.075 mm) at 4:1 molar ratio (Harrington, 1963).

The comparatively coarse SiO_2 particles are surrounded by fine-grained Na_2CO_3. The surface reaction releases CO_2 and produces a thin layer of solid Na_2SiO_3 (melting point 1088 ^oC) which separates the two reaction components and thus slows down the reaction progress. The reaction then goes on so that the ion Na^+ and O^{2-} (after separation of CO_2) diffuse towards the Na_2SiO_3-SiO_2 boundary and react there with SiO_2. The later stage of the reaction is a dissolution of unreacted quartz grains which takes almost all the time of the melting process (up to 90 % of the batch-free time). The SiO_2 concentration gradient between grain surface and the melts is relatively low in this stage. The oxygen ions are less mobile than Na^+, however, for reasons of electroneutrality, the $2Na^+:O^{2-}$ ratio has to be maintained, so that the effective diffusion coefficient will probably be close to D_O2-. Such model is suitable for application of the kinetic equations known in the field of solid phase reactions, namely the solution of Fick's law for diffusion through the spherical layer of a product. The solution by Ginstling-Brownstein yielded an activation energy of 348 kJ/mol (83 kcal/mol), which corresponds to a substantial growth of reaction rate with temperature. The rate constant is indirectly proportional to the square of initial particle size r_o^2; for the case of fine mixtures, the reaction is completed within the order of hours (see Fig. 2.7). The reaction rate increases as soon as the first melt appears. As indicated by the phase diagram of the system Na_2O-SiO_2 (see Fig. 2.8).

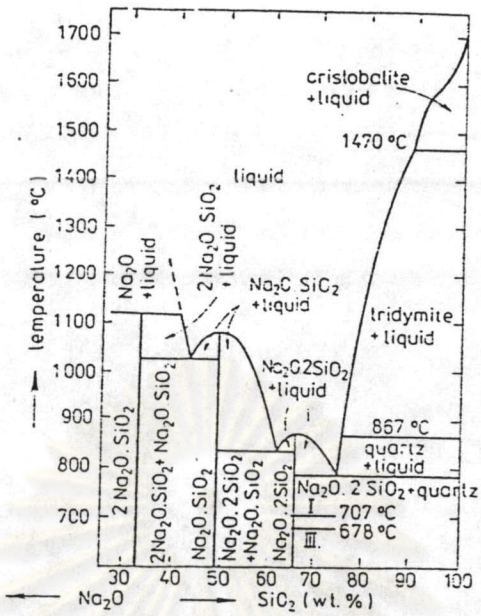

Fig. 2.8 Phase diagram of the system Na_2O-SiO_2 (Kracek, 1930, 1939).

This takes place at 790 °C and the resulting eutectic contains 73% of SiO_2. The main effect of the melt is that it improves the contact area of the reaction components. The reaction product melts at still higher temperature (above 1088 °C) and the remaining so far unreacted SiO_2 begins to dissolve in the melt while liberating the residual CO_2. Analogously, the reaction with saltpeter and sulfate can be formulated as

$$2NaNO_3 + nSiO_2 \text{ -----> } Na_2O.nSiO_2 + N_2 + (5/2)O_2,$$

$$Na_2SO_4 + nSiO_2 \text{ -----> } Na_2O.nSiO_2 + SO_2 + (1/2)O_2.$$

Sodium sulfate melts at 844 °C and in the pure state does not considerably decompose below 1500 °C. With SiO_2 it begins to react from about 1200 °C upwards, higher by several hundred degrees than Na_2CO_3. According to the reaction between sulfate and coal, it begins

to occures from 600 ^{o}C upwards producing various intermediate products (e.g. Na_2S, Na_2S_2, $Na_2S.2SiO_2$). The reaction with SiO_2 may be described by the general equation;

$$nSiO_2 + 2Na_2SO_4 + C \text{ -----> } 2Na_2O.nSiO_2 + 2SO_2 + CO_2$$

The reaction of Na_2S is more complex. It proceeds via the formation of sulphosilicates the nature of which depend on the initial sulfate to coal ratio. Excess Na_2SO_4 converts the Na_2S according to

$$3Na_2SO_4 + Na_2S \text{ -----> } 4Na_2O + 4SO_2$$

depending on the ratio of sulfate to sulfide present in the batch. With Na_2O reacting further to form sodium silicates, the number of potential reactions may be confusingly large. However, inspite of the initial excess of Na_2O, thermodynamic stability favors the formation of the metasilicate and the disilicate. That is why the primary melts due to sodium silicate reactions can be expected to occur in the sub-system $Na_2O.SiO_2$ - $Na_2O.2SiO_2$ always. The binary system $Na_2O.SiO_2$ is shown in figure 2.9. It is very well investigated. Even viscosity data are available. The main features of the corner compounds of the meta-silicate-disilicate sub system are summarized in table 2.2. The inter-mediate eutectic occurs at 837 ^{o}C. In the vicinity outside of the sub-system, a eutectic at 1022 ^{o}C occures on the sodium-rich side; a eutectic (800 ^{o}C), a liquidus reaction point (808 ^{o}C), and a sub-liquidus reaction point (700 ^{o}C) occur in the immediate vicinity outsides on the silica-rich side.

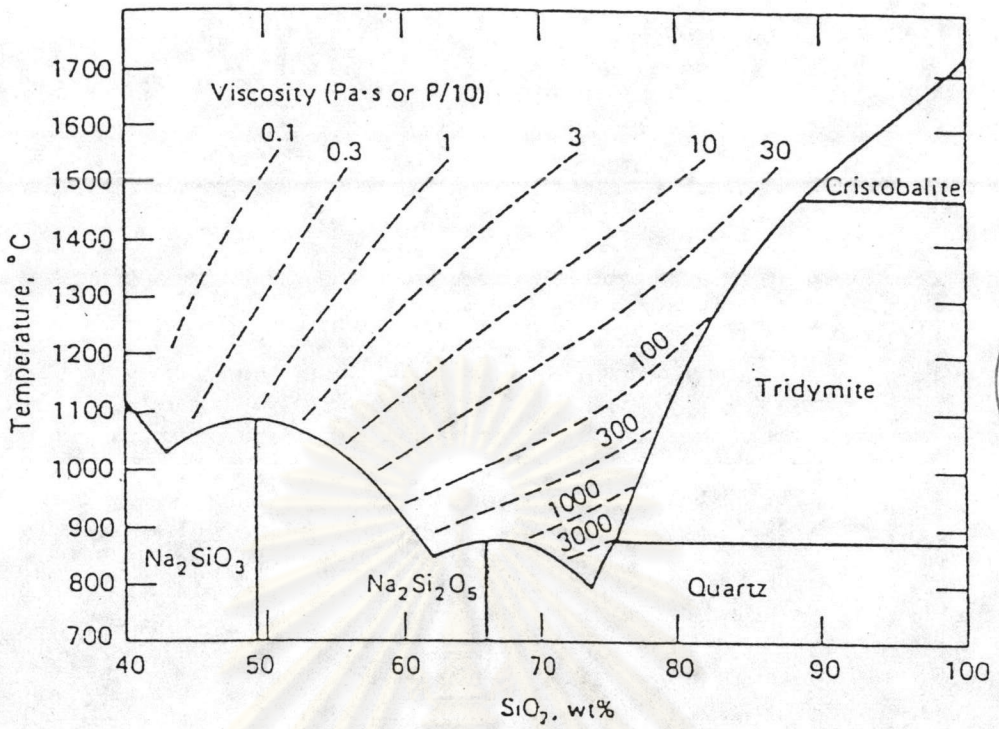

Fig. 2.9 Phase diagram of the system Na_2O-SiO_2, silica-rich range; for the liquid phase, iso-viscosity lines in Pa.s are given (by multiplication with 10, the familiar unit in dPa.s is obtained); after Mark, and Othmer, (1982).

Tab 2.2 Properties of $Na_2O.SiO_2$ and $Na_2O.2SiO_2$; Molar mass M, liquidus temperature T_{liq}, enthalpy of melting H_{melt}, heat content H_o referred to 25 °C, and viscosity n at T = T_{liq}

compound	M in g/mol	T_{liq} in °C	H_{melt} in KW/t	H_o (1000°C) in KWh/t	log n,n in dPa.s
$Na_2O.SiO_2$	105.998	1089	77.8	424.0	+1
$Na_2O.2SiO_2$	80.995	874	50.1	458.4	+3.5

The viscosity data of some sodium silicate melts are again given in table 2.2. For the low-melting compound $Na_2O.SiO_2$, log n is already quite high. The viscosity of the compounds in table 2.2 may be estimated by the Stokes-Einstein relation

$$\log n \sim \log R.T/(6nDLr)$$

L ~ 6×10^{23} mol^{-1}, D = diffusion coefficient ~ 1×10^{-6} cm^2/s, r = size of the molecular unit. The size r can be estimated by the molar volume $V_m = M/\rho$, i.e., by $r = (LV_m)^{1/3}$. The above equation fails to give reasonable estimates for polymerizing melts (like silicate melts), but works fairly well for melts with ionic character. Viscosity of these melts have $\log n \leq 0$.

Sodium silicates further react in the batch to form ternary compounds, mainly in the system Na_2O-CaO-SiO_2. Its phase diagram (see Fig. 2.10 at the next page) exhibits a number of low-temperature invariant points. Their properties are summerized in table 2.3. Note the quite high viscosities of these ternary melts.

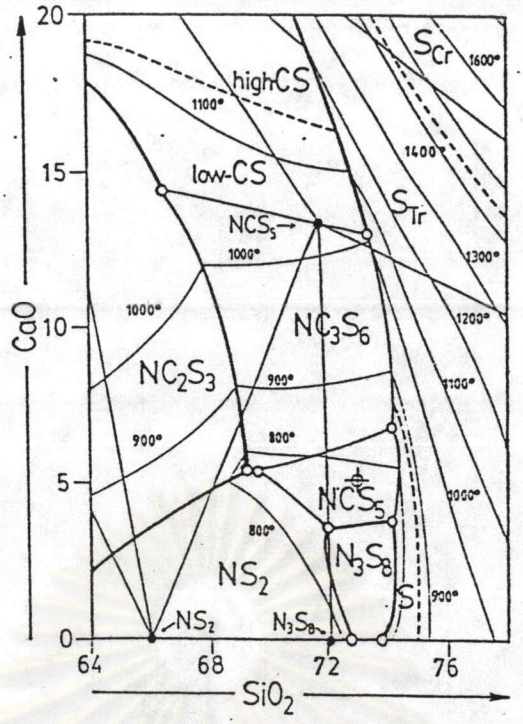

Fig. 2.10 Phase diagram of the system Na_2O-CaO-SiO_2 in the technically relevant range, redesigned by Conradt (1992) after data from Leven, Robin, and McMurdie (1964 and 1969).

Tab. 2.3 Properties of selected invariant point in the technologically relevent part of the system Na_2O-CaO-SiO_2; meta = metastable eutectic, EU = eutectic, R = reaction point, n = viscosity at $T = T_{inv}$

invarient point	T_{inv} in °C	composition in wt. %	log n, n in dPa.s
NS_2-NC_3S_6-S (meta)	765	73.0 SiO_2, 5.0 CaO, 22.0 Na_2O	5.7
N_3S_8-NCS_5-S (EU)	755	74.2 SiO_2, 3.8 CaO, 22.0 Na_2O	5.9
NCS_5-NC_3S_6 (R)	827	74.1 SiO_2, 7.0 CaO, 18.9 Na_2O	5.4
NS_2-NCS_5-NC_3S_6 (EU)	755	72.2 SiO_2, 3.6 CaO, 24.3 Na_2O	5.6
NS_2-N_3S_8-NCS_5 (R)	785	69.6 SiO_2, 5.3 CaO, 25.1 Na_2O	5.0

2.2.3 The soda lime reaction and further reactions

Na_2CO_3 forms a low temperature eutectic with $CaCO_3$ followed by a low-temperature reaction point ("double salt formation") Respective temperatures can be read from Fig. 2.11,

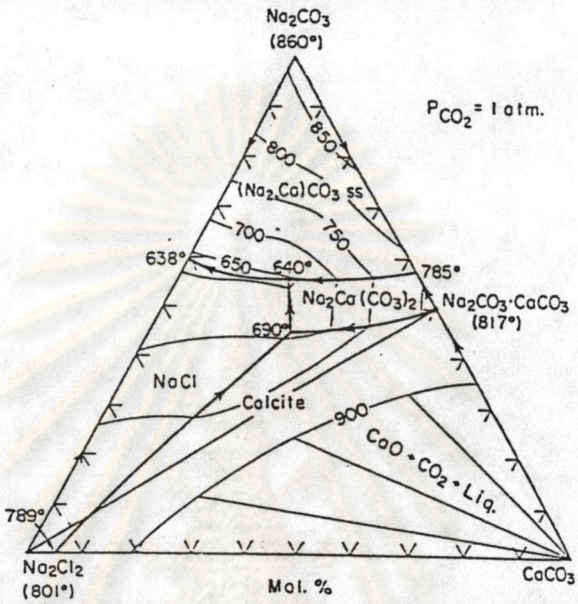

Fig. 2.11 Phase diagram of the system $NaCl-Na_2CO_3-CaCO_3$ after Levin et al., (1964, 1969) showing the interaction between soda ash and limestone.

this reaction is meaningful in so far as is competes with the soda-quartz reaction path towards the ternary silicates, e.g.,

$$Na_2CO_3 + Na_2Ca(CO_3)_2 + 3SiO_2 \text{ -----> } 2Na_2O.CaO.3SiO_2 + 3CO_2$$

Information on the behavior of dolomite is scant. It is known to decay within a temperature range 730 to 760 ^oC like;

$$MgCa(CO_3)_2 \text{ -----> } MgCO_3 + CaCO_3$$

In a simplified approach, Mg may be dismissed as playing a role in

promoting the formation of primary melts. It is not clear either, whether or not the $CaCO_3$ stemming from dolomite decay is able to form double salt.

Finally, the effect of feldspar is exemplarily shown in Fig. 2.12.

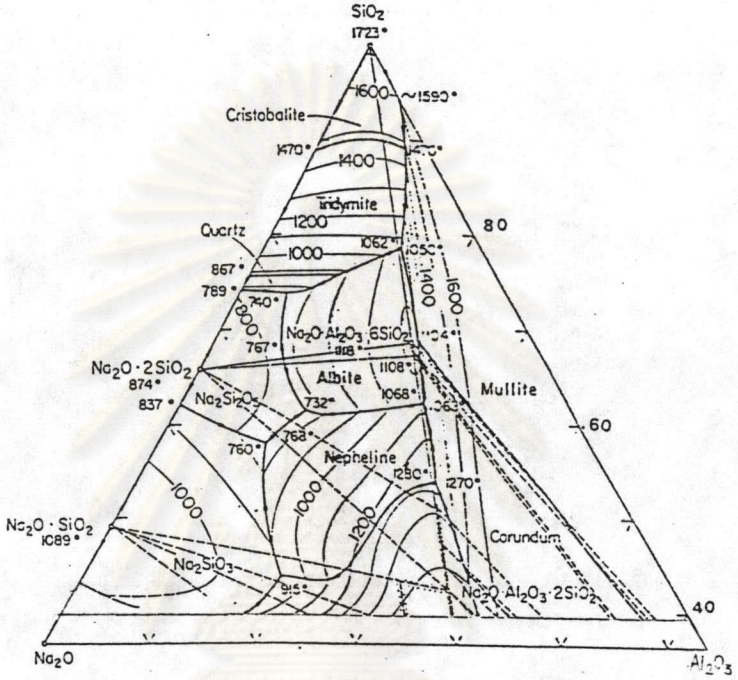

Fig. 2.12 Phase diagram of the system Na_2O-Al_2O_3-SiO_2, technically relevant range; after Levin et al. (1964 and 1969).

Three ternary eutectics at 732, 740, and 760 °C, respectively, and a binary eutectic at 767 °C are founnd in the technically relevant composition range SiO_2-$Na_2O.SiO_2$-$Na_2O.Al_2O_3.2SiO_2$. Table 2.4 summa-rizes the finding presented on the previous page.

Tab. 2.4 Summary of relevant invarient points in different systems; EU = eutectic, R = reaction point, P = peritectic, M = metastable eutectic; temperatures in °C; (2) indicates that two invarient points of the same nature and temperature exist in the system.

system	invarient point for primary melt formation
SiO_2-Na_2O	EU 788; R 798; P 874; EU 837; P;1089; EU 1022
SiO_2-CaO-Na_2O	M 765; R 827; EU 755; (2); R 785 (2); R 1040 (2)
Na_2CO_3-$CaCO_3$	EU 785; R 817
Na_2CO_3-$NaNO_3$	EU 320*
Na_2CO_3-Na_2SO_4	continuously 851 - 884
Na_2CO_3-Na_2S	EU 762
Na_2SO_4-$NaNO_3$	EU 320*
Na_2O-Al_2O_3-SiO_2	EU 732; EU 740; EU 760; P 1118

* for technically relevant molar ratios, the liquidus of the system Na_2CO_3-Na_2SO_4-$NaNO_3$ is above 800 °C

With the exception of pure $NaNO_3$, the vast majority of low-T liquid phase formation occurs within the range between 730 and 1090 °C In other words, the formation of primary melts is unlikely to occur below 730 °C, and is most likely completed at 1090 °C. At the present stage, a prediction of the predominant and relevant primary liquid phase formation in a real batch may be a difficult enterprise, and we may not be able to identify "the" quasi-isothermal reaction temperature T_R yet. We may adopt for sure nothing else but a potential onset at 730 °C and a terminal at 1090 °C. In any case, the temperature

range up to 1200 °C is sufficient to complete the entire process of batch melting of commercial soda lime glasses, and indeed liquidus temperatures, of such glasses are always located well below 1200 °C. Of course, in industrial practice, higher process temperatures are applied to complete the batch melting within reasonably short times.

2.3. Ionic mobility during liquid phase formation

As the occurence of liquid phase during batch melting is a key event, its precise observation is one of the main focuses of the presented work. Daniels (1973) briefly mentioned that conductivity measurements are suited to indicate the onset liquid phase formation, however, he did not elaborate nor give any experimental results. Indeed, conductivity is the suitable means to investigate ionic mobility, which is in turn, linked to the viscosity of the system. Because of the similarity between the mechanism of viscous flow, diffusion, and electrical conductivity, which are all activated process, a relationship between these phenomena was sought. It has been established empirically by Morey (1954) that, the temperature dependence of viscosity and resistivity of glass melts are often mutually dependent according to the relationship;

$$\log n \sim 3 \log \rho, \text{ or } \log n = a \log \rho - b$$

However, it should be born in mind that mobility of cations is critical for transfer of electric charges while mobility of anionic structural units (network former) is involved in the case of viscous flow, then this makes difficult to interpret the relation between the

two quantities. In a commercial glass batch, the predominant charge carrier is Na^+ ion; the contribution of other ions may be neglected. In solid Na salts, diffusion coefficients assume the order of 10^{-9} to 10^{-11} cm^2/s. For example, for solid NaCl, 7.5×10^{-11} cm^2/s, at 550°C and 5×10^{-9} cm^2/s at 750 °C are found. In the liquid phase, diffusion coefficients in the order of 10^{-6} cm^2/s are typical. In the vicinity below the liquidus temperature T_{liq}, an abrupt increase (cross over) of the temperature coefficient of D from impurity to thermally activated diffusion occurs. The Nernst-Einstein relation gives as estimate for corresponding conductivity X in $(ohm\text{-}cm)^{-1}$ by

$$D = X.R.T.\Gamma.M/(Z^2.F^2.x.\rho)$$

where R is gas constant, F is Faraday's constant, T is the absolute temperature, and ρ is density of the system; x, z, and M are molar fraction, charge number, and molar mass of the predominant charge carrier; Γ is the thermodynamic factor of the corresponding component. None of the variables T, Γ, x, and ρ varies except within the same order of magnitude. Thus the direct proportionality $D \propto X$ approximately holds, and liquid phase formation is expected to yield an increase of conductivity by approx. three order of magnitude. Such a significant drop is expected to appear very clearly even if we allow for large errors in the absolute determination of X.

A suitable method for measuring the electrical conductivity of glass melts up to 1450 °C has been described by Stanek et al., (1965). An AC source of 800 Hz frequency was used to eliminate polarization, and platinum electrodes were employed.